

Leaching Kinetics of Valuable Metals from Calcined Material of Spent Lithium-Ion Batteries

Natcha Wongnaree, Tapany Patcharawit, Tanongsak Yingnakorn, and Sakhob Khumkhoa*



Cite This: ACS Omega 2024, 9, 46822–46833



Read Online

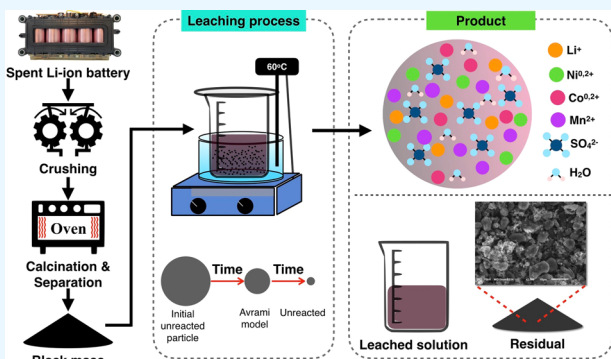
ACCESS |

Metrics & More

Article Recommendations

Supporting Information

ABSTRACT: This study aimed to investigate the leaching kinetics of valuable metals contained in the calcined black mass derived from the incineration of spent lithium-ion battery (LIB) modules. The effects of sulfuric acid (H_2SO_4) concentration (0.5–3 M), hydrogen peroxide (H_2O_2) concentration (0.5–2.0 vol %), solid/liquid (S/L) ratio (25–75 g/L), leaching time (10–120 min), and leaching temperature (30 °C–70 °C) on metal leaching efficiency from black mass were investigated. The optimal leaching conditions were achieved with 1 M H_2SO_4 , 1 vol % H_2O_2 , and a S/L ratio of 50 g/L at 60 °C for 60 min. Under these conditions, Li, Ni, and Mn had leaching efficiencies of 100%, with Co at 97.17%, respectively. An investigation of the leaching kinetics utilizing H_2O_2 as an additive revealed that the Avrami model fits the metal leaching process. The results of this study suggested that diffusion and surface chemical reactions controlled the leaching mechanisms of these metals, with activation energies of 7.829, 5.646, and 5.077 kJ mol⁻¹ for Li, Ni, and Co, respectively.



1. INTRODUCTION

Lithium-ion batteries (LIBs) are widely used in electronic devices such as mobile phones, laptops, cameras, and electric vehicles (EVs).^{1–3} The economic growth of EVs is expected to accelerate over the next 25 years, increasing from the forecasted 7 million in 2022 to 180 million in 2045.⁴ LIBs provide several distinct advantages over other battery types, notably, high specific energy density, high power density, lightweight construction, long cycle life, and rapid charging capability,^{5–7} thus playing a crucial role in various technological applications.

LIBs are structured with two electrical terminals: an anode (negative electrode) and a cathode (positive electrode). The anode is comprised of a copper foil substrate coated with graphite, while the cathode consists of an aluminum foil substrate coated with various lithiated mixed transition metal oxides such as $LiCoO_2$ (LCO), $LiNiO_2$ (LNO), $LiMnO_2$ (LMO), $LiFePO_4$ (LFP), and $LiNi_xCo_yMn_zO_2$ (NMC) (where $x+y+z = 1$). Thus, the cathode contains valuable metals, such as Li, Ni, Co, and Mn.^{8–10} In addition, LIBs exhibit an average operational lifespan ranging from 8 to 10 years within the context of EVs, with a substantial escalation in the accumulation of spent LIBs projected to yield a volume of 4 million tons by 2024.¹¹ Spent LIBs are considered harmful to human, animal, and environmental health due to the presence of heavy metals and organic chemicals (electrolytes and separators). Therefore, recycling of spent LIBs can reduce these problems and facilitate the recovery of valuable metals.^{12,13}

Effective recycling methods for spent LIBs include pyrometallurgy, hydrometallurgy, and direct regeneration.^{14,15} The pyrometallurgical process consists of melting spent LIBs into an alloy. The alloy can be further refined into pure products via hydrometallurgy. However, pyrometallurgy requires high energy consumption, emits hazardous air pollutants, and has lower product purity than that achieved via alternative methods due to the formation of slag byproduct.^{16,17} By contrast, hydrometallurgy stands out as a prominent metallurgical process renowned for its environmental sustainability, lower energy consumption, production of high-purity metals, and high recovery efficiency.^{18–21} Leaching is a key step in the hydrometallurgical process. This process involves extracting metals from a solid substrate using inorganic (e.g., sulfuric (H_2SO_4), nitric (HNO_3), and hydrochloric (HCl) acids) or organic (e.g., oxalic, citric, and lactic acids) acids.^{22–24} Inorganic acids exhibit high leaching efficiency for certain metals (Li, Al, and Cu); however, Co, Ni, and Mn possess stable oxidation states (Co^{3+} , Ni^{3+} , and Mn^{4+}) that make them less soluble in such reagents. Consequently, metals with a high oxidation state must be

Received: May 30, 2024

Revised: October 31, 2024

Accepted: November 7, 2024

Published: November 12, 2024



Table 1. Experimental Variables and Results of Leaching Spent LIB Cathode Materials with H₂SO₄ and H₂O₂

Sample	H ₂ SO ₄ (M)	H ₂ O ₂ (vol %)	S/L (g/L)	Temp (°C)	Time (h)	Leaching efficiency	ref
NMC 111	1	1	40	40	1	99.7% Li/Co/Mn/Ni	27
NMC	2	5	100	60	2	99% Li/Co/Mn/Ni	28
NMC 811	2	3	50	50	1	100% Li/Co/Mn/Ni	29
LCO and NMC 111	2	10	33	70	3	99.76% Li, 98.46% Co, 98.62% Mn, 98.56% Ni	1
Mixed LIBs	2	4	100	70	4	98.8% Li, 99.6% Co, 97.8% Mn, 99.4% Ni	12
NMC 111	1.5	8	30	25	1	80.2% Li, 93.2% Co, 90.3% Mn, 91.5% Ni	30
LCO, Li ₂ CoMn ₃ O ₈ and (Li _{0.85} Ni _{0.05}) (NiO ₂)	1	5	50	95	4	93.4% Li, 79.2% Co, 84.6% Mn, 96.3% Ni	31
NMC 111, LCO and LMO	2	2	50	80	1	81% Li, 98.2% Co, 97.1% Mn, 98.7% Ni	32

converted to a lower oxidation state (Co²⁺, Ni²⁺, and Mn²⁺) using a reducing agent such as hydrogen peroxide (H₂O₂), ascorbic acid, or sodium bisulfite.^{14,25,26}

The leaching of cathode materials composed of Li, Ni, Mn, and Co (NMC) using a combination of H₂SO₄ and H₂O₂ has been well studied, as shown in Table 1. These investigations focused on crucial parameters such as H₂SO₄ and H₂O₂ concentrations, solid-to-liquid (S/L) ratio, and leaching temperature and time. The results indicated that a H₂SO₄ concentration of 1–2 M, H₂O₂ concentration of 1–10 vol %, S/L ratio of 30–100 g/L, leaching temperature of 25 °C–100 °C, and leaching time of 1–4 h. These experimental conditions provided leaching efficiencies greater than 80% for Li, Ni, Mn, and Co metals from NMC.

Additionally, investigations have been conducted to determine the optimal leaching conditions for LIBs, with many researchers studying the leaching kinetics. Such studies have explained the leaching kinetics by fitting the reacted shrinking core and Avrami models.^{33–35} For example, Sahu et al. (2023) studied the leaching kinetics of LCO cathodes using 0.8 mol/L ascorbic acid and a S/L ratio of 50 g/L at 70 °C for 60 min.¹⁰ The results indicated high leaching efficiencies of nearly 100% for Li and Co. The low activation energy (E_a) values for these metals suggested a good match with the surface chemical reaction model. Additionally, Yang et al. (2022) investigated the leaching kinetics of NMC cathode powder using 2.5 mol/L H₂SO₄, 20 g/L oxalic acid, and a S/L ratio of 1 g/10 mL at 85 °C for 100 min. The leaching process resulted in high Li, Ni, Mn, and Co leaching efficiencies greater than 96%.³⁶ The leaching kinetics for these metals were well-described by the Avrami model, with E_a values ranging from 31 to 48 kJ/mol, indicating that leaching of Li was primarily controlled by diffusion, while Ni, Mn, and Co metal leaching were controlled by surface chemical reactions. The study conducted by Gao et al. (2018) examines the recycling of NMC using weak acidic leachate. Optimal leaching conditions are found to be at an acetic acid concentration of 3.5 mol/L, at 60 °C, and 4 vol % H₂O₂ as a reductant. The reductant shifts the rate-determining step from ion diffusion to surface chemical reactions, improving efficiencies (nearly 100 wt % of leaching rates). Kinetics analysis reveals activation energies for Li, Ni, Mn, and Co values ranging from 52 to 56 kJ/mol.²⁵ Research carried out by Meshram et al. (2015) investigated the recovery of valuable metals from spent LIBs using H₂SO₄ leaching and a reducing agent additive, sodium bisulfite (NaHSO₃). The optimal conditions were identified as 1 M H₂SO₄ and 0.075 M NaHSO₃ at 368 K, with a S/L ratio of 20 g/L for 4 h. Under these conditions, the leaching efficiency achieved was more than 90% for Li, Co, and Ni and 87.9% for

Mn. The dissolution kinetics of the metals followed a logarithmic rate law, suggesting a chemical control mechanism. E_a derived from Arrhenius plots values ranging from 20 to 27 kJ/mol (Li, Ni, and Co).²⁶ Previous research in this area has focused on the leaching and kinetics of spent LIB cathode materials such as NMC, LCO, LMO, and black mass. However, black mass separation can be isolated through various separation techniques, such as mechanical separation and calcination.^{37,38} The raw material black mass used in this study was obtained via a calcination treatment process at about 500 °C. This temperature regime effectively decomposes organic components and pyrolysis binders (e.g., polyvinylidene fluoride, polytetrafluoroethylene), thereby facilitating the separation of black mass from other components (e.g., current conductors and battery casing).^{37–39} Therefore, unlike previous studies, the incinerated black mass from spent LIBs in this study is heavily contaminated with aluminum compounds, carbon from the graphite anode, and decomposed organic and binder materials. The differences with this material, such as the complex chemical composition and crystal structures compared with those investigated in previous studies, could suggest a potential deviation in E_a values when observed under leaching kinetics analysis. The focus of this research is to study the leaching behavior of the material using sulfuric acid, with and without the addition of H₂O₂ as an additive, to determine the optimal combination of acid and the additive. By optimizing the use of acid and the additive, the recovery of NMC-based materials can be enhanced, minimizing the recycling costs and also reducing secondary waste generation. The experimental method was designed to investigate the effects that certain critical parameters have on the leaching process, such as reaction time, acid concentration, pulp density, amount of the additive, and temperature. Additionally, this study employs the unreacted shrinking core and Avrami models to investigate the leaching kinetics of LIB cathode material, thereby enhancing the understanding of the leaching process mechanism.

2. EXPERIMENTAL METHODS

2.1. Materials and Reagents. The black mass separated from the calcined materials of spent LIBs was used as the raw material for this study. The chemical reagents used in the leaching process were of analytical grade and procured from Quality Reagent Chemical Co. Ltd. (Mueang Chon Buri, Thailand), including HCl (37% purity), H₂SO₄ (98% purity), HNO₃ (69% purity), and H₂O₂ (35% purity). Dilution of chemical reagents was performed with deionized water to prepare any requisite solutions.

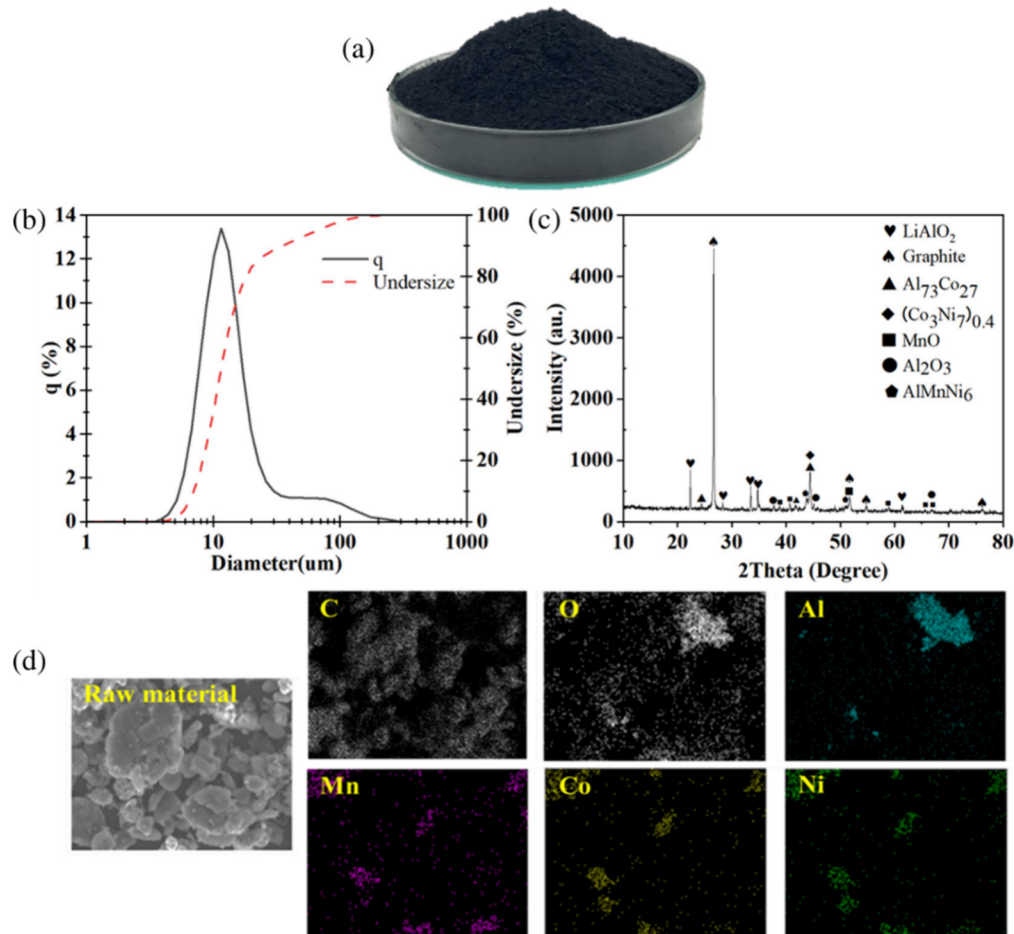


Figure 1. Analysis of black mass separated from calcined material of spent LIBs: (a) black mass sample, (b) particle size distribution of the black mass sample, (c) XRD pattern of the black mass sample, and (d) elemental map of elements in the black mass sample.

2.2. Leaching Method. The investigated parameters of this study included H_2SO_4 concentration (0.5–3 M), H_2O_2 concentration (0.5–2 vol %), S/L ratio (25–75 g/L), temperature (30 °C–70 °C), and leaching time (10–120 min). The leaching experiments were conducted under controlled conditions in a 600 mL beaker covered with a watch glass to regulate vapor loss. The solution volume was maintained at least 95% of the total volume, with a solution volume of 200 mL and a solid mass range of 5–15 g. A water bath, consisting of a crystalline dish equipped with an electronic contact thermometer, was employed for precise temperature control. The raw material and liquid mixture were continuously stirred using a magnetic stirrer until uniformity was achieved. Following the leaching process, a vacuum pump filter system was employed to separate the solid and liquid phases, including a flask, Büchner funnel, and vacuum pump. The leaching efficiency of the metals was calculated using eq 1:

$$\text{Leaching efficiency of metal (\%)} = \frac{\text{Metal dissolved in the leachant}}{\text{Total content of metal in the raw material}} \times 100 \quad (1)$$

2.3. Analytical Method. The metal ion concentrations in the raw material and leaching solutions were quantitatively analyzed via inductively coupled plasma-optical emission spectrometry (ICP-OES) using an Optima 8000 instrument (PerkinElmer, Waltham, MA, USA). Before ICP-OES analysis,

the solid samples were prepared by digesting 1 g of the sample in 40 mL of aqua regia (a 3:1 ratio of HCl and HNO_3) and heating to boiling for 40 min. After cooling to room temperature, the solution was filtered into a 100 mL volumetric flask, subsequently diluted to a final volume of 100 mL, and then diluted to the established calibration range. The solid compounds were characterized by X-ray diffraction (XRD) using a D2 Phaser diffractometer (Bruker, Billerica, MA, USA) within the 2-theta range of 10°–80° at 0.02° step size. The morphological characteristics of the sample were assessed via scanning electron microscopy coupled with energy-dispersive X-ray spectroscopy (SEM-EDS) using a JSM-6010LV instrument (Jeol Ltd., Tokyo, Japan). The particle size distribution of the raw material was analyzed by laser diffraction particle size analysis performed using an LA-950 V2 instrument (Horiba, Kyoto, Japan). X-ray absorption spectroscopy (XAS) was utilized to gain insights into the local environment and electronic states of the elements present in the raw material.

3. RESULTS AND DISCUSSION

3.1. Raw Material Characterization. The black mass separated from the calcined material of spent LIBs (obtained from a Thai company) was black in color and a coarse powder, as shown in Figure 1a. The calcination process was employed at about 500 °C. This temperature facilitated the decomposition of organic matter and binder,^{37,40} resulting in a

Table 2. Chemical Composition of Black Mass from Spent LIBs

Sample	Element (wt %)					
	Li	Co	Ni	Mn	Al	other
Raw material	3.47	10.16	11.82	4.04	4.22	66.29

sufficient separation. In contrast, the calcination at higher temperatures (e.g., 700 °C) led to several drawbacks, such as scraps exhibiting increased fragility, the active materials becoming contaminated with aluminum foils due to the metal's low melting point,³⁸ increased energy consumption, and altering the structure of metal compounds.⁴¹ The average mean size (D_{90}), mode size (D_{10}), and median size (D_{50}) of the black mass particles, as shown in Figure 1b, were 40.556, 7.059, and 11.762 μm, respectively. The XRD analysis revealed that the black mass was composed of graphite, Li–Al oxide, Al–Co, Co–Ni, Mn oxide, and other constituents, as shown in Figure 1c. These metal alloys and oxides were distributed throughout the bulk of the material, as demonstrated by EDS

mapping (Figure 1d). However, Li could not be identified due to its lightweight nature and the use of low X-ray energy in the analysis. The chemical composition of black mass (determined using ICP-OES) included 3.47 wt % Li, 10.16 wt % Co, 11.82 wt % Ni, 4.04 wt % Mn, and 4.22 wt % Al, with trace elements (Table 2).

XAS was employed to infer the metal oxidation states of the black mass, specifically using the K-edge X-ray absorption near edge structure (XANES) and extended X-ray absorption fine structure (EXAFS) techniques, as shown in Figure 2. The Ni K-edge XANES spectrum of the black mass revealed similarities with that of the Ni foil reference, but the absorption intensity was greater for Ni foil and less for the NiO reference. This suggested that the Ni mean oxidation state in the studied material was within the range of 0 and +2, as shown in Figure 2a. The corresponding EXAFS spectrum in Figure 2b displays the radial distances. The first peak, at approximately 1.2 Å, was associated with Ni–O interactions, while the second peak, at approximately 2.2 Å, was correlated with Ni–Ni interactions. Figure 2c presents the XANES spectrum of Co in the black

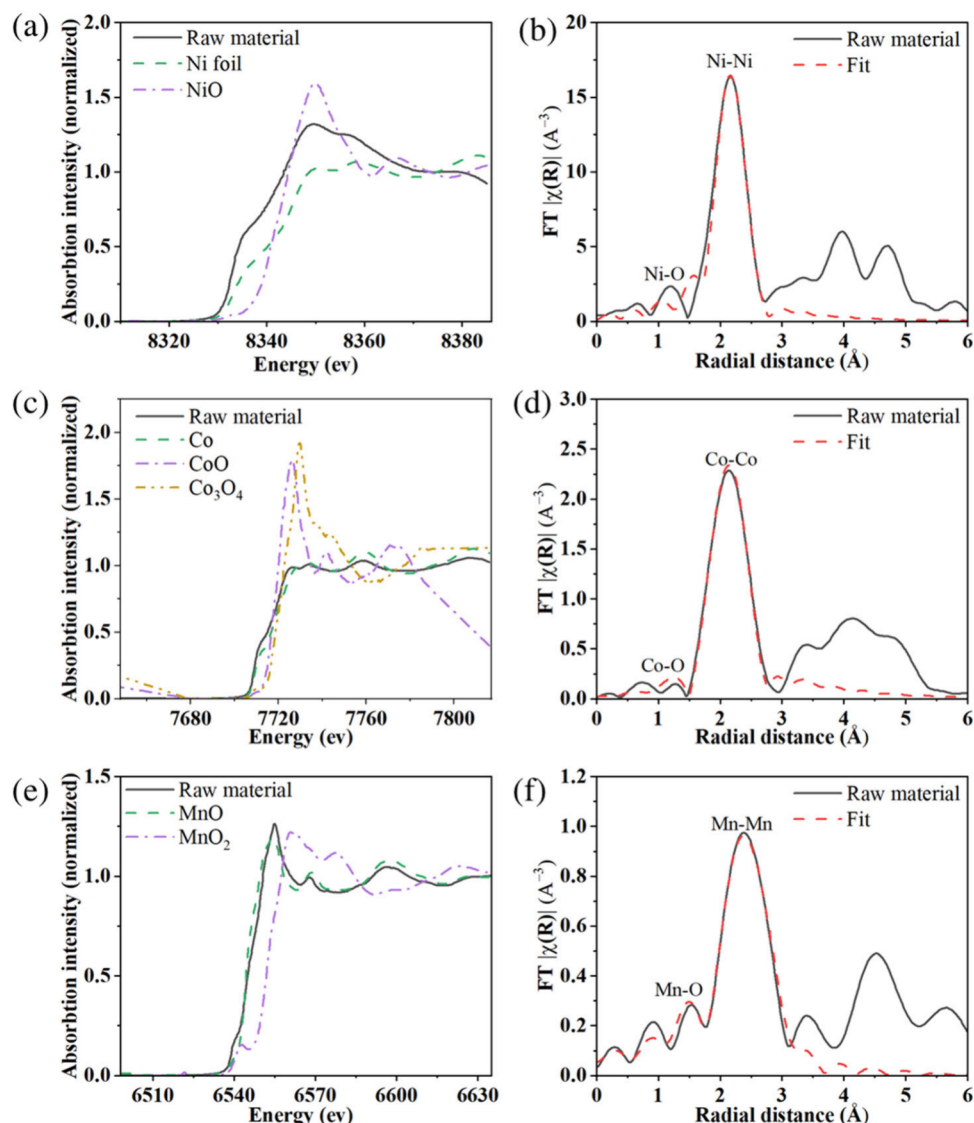


Figure 2. XAS analysis of black mass separated from calcined material of spent LIBs. (a) Ni K-edge XANAFS spectra. (b) FT EXAFS spectra of Ni. (c) Co K-edge XANAFS spectra. (d) FT EXAFS spectra of Co. (e) Mn K-edge XANAFS spectra. (f) FT EXAFS spectra of Mn.

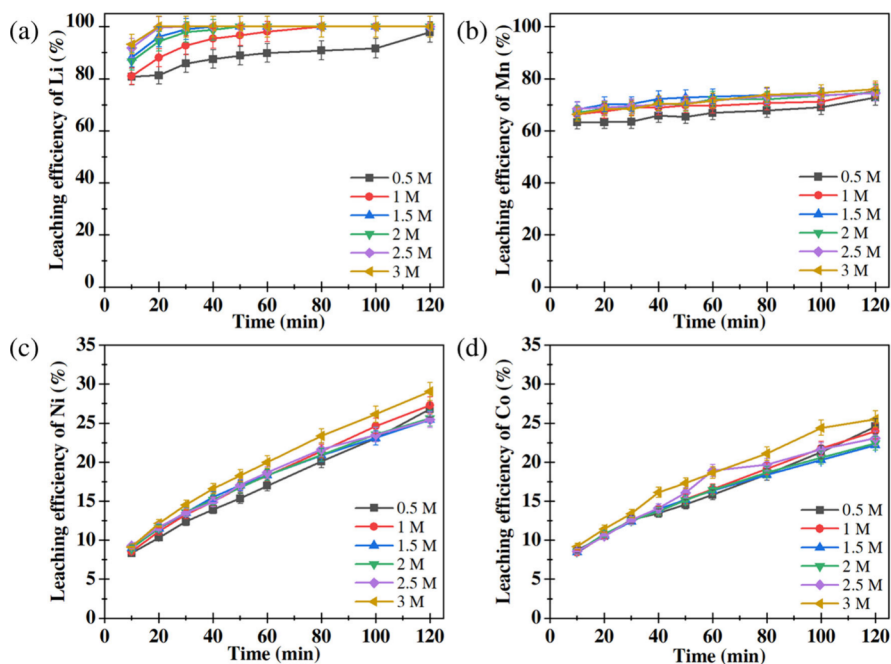


Figure 3. Leaching efficiency of metals with different H_2SO_4 concentrations and a S/L ratio of 50 g/L at 30 °C: (a) Li, (b) Mn, (c) Ni, and (d) Co.

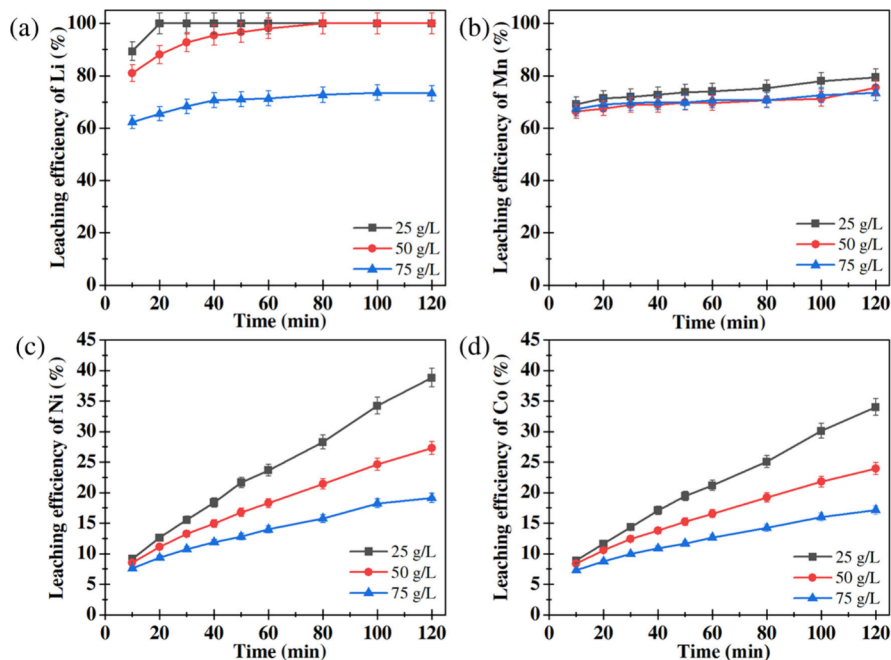


Figure 4. Leaching efficiency of metals with different S/L ratios and 1 M H_2SO_4 at 30 °C: (a) Li, (b) Mn, (c) Ni, and (d) Co.

mass compared with reference materials (Co, CoO, and Co_3O_4). The spectrum of Co in the black mass was similar to that of the Co reference, indicating that an oxidation state of 0 was most likely. However, it was not entirely 0, with some portions exhibiting an oxidation state of +2. The EXAFS spectrum, as shown in Figure 2d, indicated Co–O interactions at a radial distance of approximately 1.3 Å, and a second peak corresponded to Co–Co interactions at a radial distance of approximately 2.3 Å. As shown in Figure 2e, the XANES spectrum of Mn in the black mass was more similar to that of the MnO than MnO_2 reference materials, indicating a likely oxidation state of 2. The EXAFS data in Figure 2f indicated Mn–O and Mn–Mn bond distances of approximately 1.6 and

2.4 Å, respectively. The observed characteristics of the calcined black mass suggest a significant alteration in the chemical structure from the pretreated black mass (original compound).

3.2. Optimization of Black Mass Leaching. The black mass is a coarse powder containing valuable metals and graphite. However, it is difficult to solubilize all the valuable metals in black mass using standard acids without optimizing the leaching conditions. Thus, by optimizing the leaching conditions of the black mass, the valuable metals can be recovered from the black mass for further processing. This study investigated the influence of various leaching process parameters on the extraction of valuable metals (Li, Mn, Ni, and Co) from black mass, including H_2SO_4 concentration, S/L

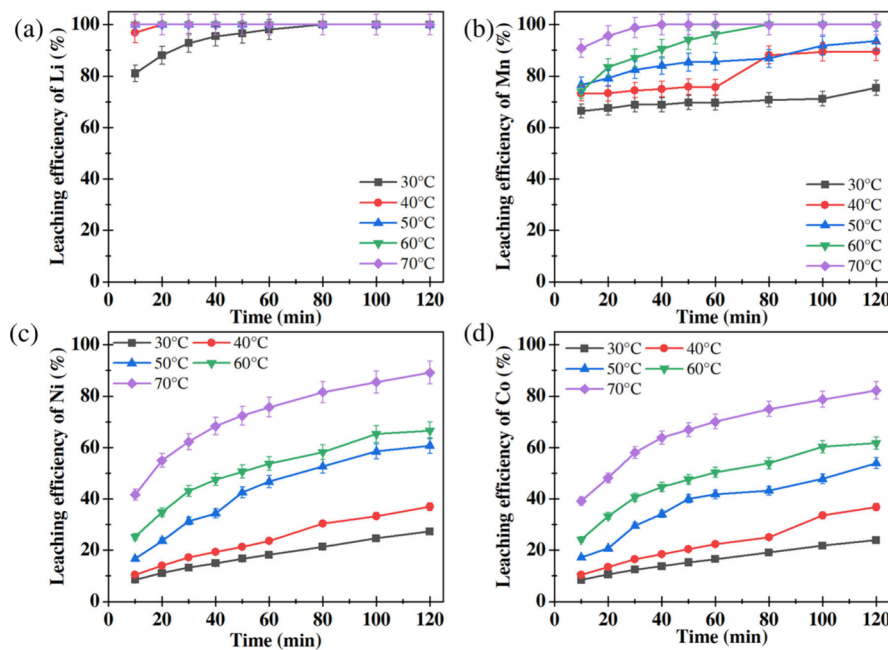


Figure 5. Leaching efficiency of metals at different temperatures with 1 M H_2SO_4 and a S/L ratio of 50 g/L: (a) Li, (b) Mn, (c) Ni, and (d) Co.

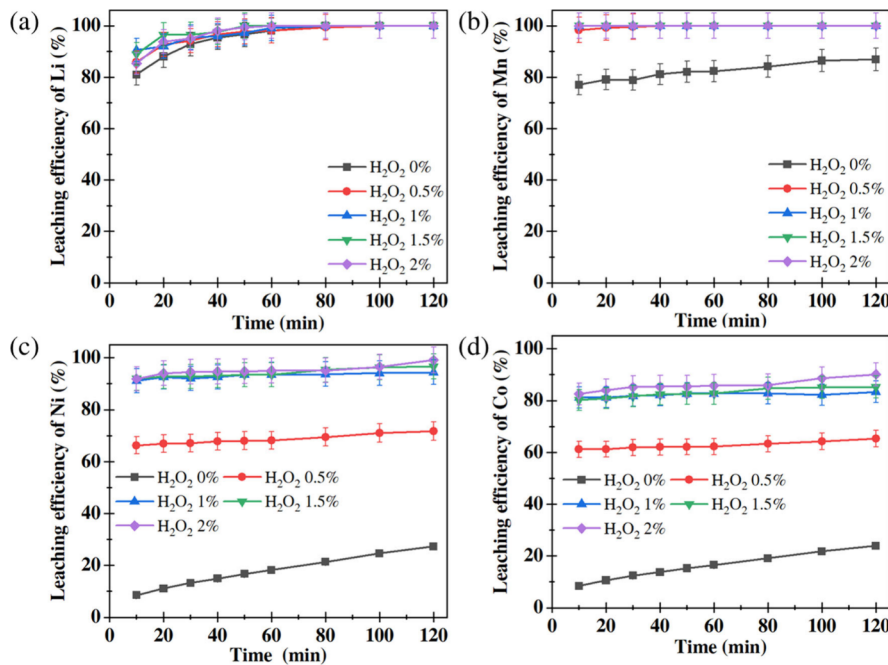


Figure 6. Leaching efficiency of metals with different H_2O_2 concentrations, 1 M H_2SO_4 and a S/L ratio of 50 g/L at 30 °C: (a) Li, (b) Mn, (c) Ni, and (d) Co.

ratio, temperature, and H_2O_2 concentration. To optimize the H_2SO_4 concentration, leaching experiments were conducted at a constant S/L ratio (50 g/L), temperature (30 °C), and leaching time (120 min), with the H_2SO_4 concentration varying between 0.5 and 3 M (Figure 3). The results revealed that 1–3 M H_2SO_4 led to a rapid initial Li leaching rate, with greater than 80% leaching efficiency achieved within the first 10 min, which approached 100% after 80 min. Conversely, a lower H_2SO_4 concentration (0.5 M) achieved a lower leaching efficiency within the duration of the experiment. Leaching of other metals (Mn, Ni, and Co) exhibited differing behaviors. While not completely dissolved, these metals achieved leaching

efficiencies of approximately 70% for Mn, 25% for Ni, and 20% for Co at 80 min, which remained relatively constant throughout the experiment. Consequently, 1 M H_2SO_4 was selected based on its capacity to achieve an optimal Li leaching efficiency of 100% while minimizing acid consumption.

Optimization of the S/L ratio was investigated from 25 to 75 g/L while maintaining constant conditions of 1 M H_2SO_4 and 30 °C (Figure 4). The results indicated that complete Li leaching was achieved within 80 min at S/L ratios of 25 and 50 g/L, whereas higher ratios induced leaching efficiencies less than 80%. Hence, a S/L ratio of 50 g/L was selected for subsequent experiments. However, complete leaching effi-

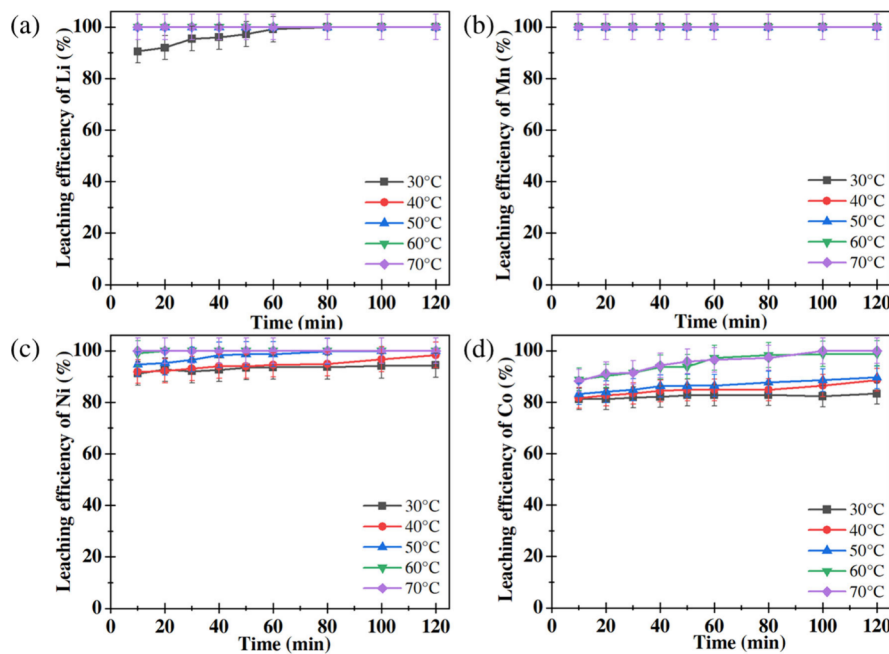


Figure 7. Leaching efficiency of metals at different temperatures with 1 M H₂SO₄, S/L ratio of 50 g/L, and 1 vol % H₂O₂: (a) Li, (b) Mn, (c) Ni, and (d) Co.

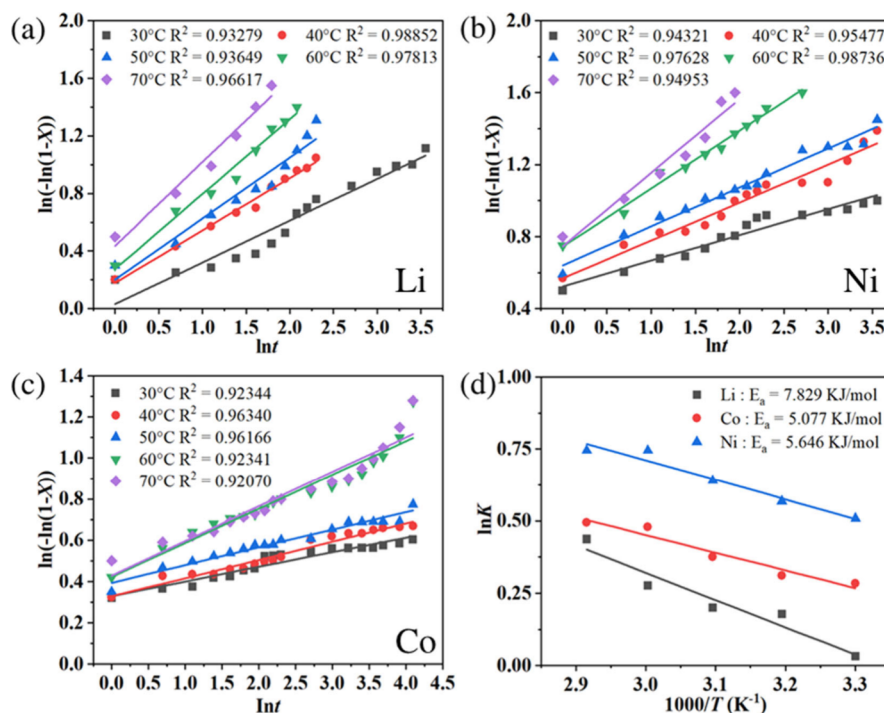


Figure 8. Fitting of the leaching kinetics data by the Avrami model in the presence of H₂O₂: (a) Li, (b) Ni for initial 10 min, (c) Co for initial 60 min, and (d) Arrhenius plot.

ciency for Mn, Ni, and Co was not achieved under these conditions, necessitating an increase in temperature. As shown in Figure 5, increasing the temperature to 70 °C substantially enhanced Mn, Ni, and Co leaching efficiencies (>80%).

The effect of varying the H₂O₂ concentration from 0.5 to 2 vol % on metal leaching efficiency was investigated and explored. Experimental conditions (S/L ratio of 50 g/L and 1 M H₂SO₄ at 30 °C for 10–120 min) were maintained and kept constant throughout the experiment, as shown in Figure 6.

Rapid reactions were observed, with Li leaching efficiency approaching 100% at 60 min, as shown in Figure 6a. Mn leached the fastest, with nearly 100% leaching efficiency achieved within 10 min for 0.5–2 vol % H₂O₂ concentration (Figure 6b). Adding H₂O₂ had an overall effect in accelerating the reaction rate, with Mn being the most susceptible out of all the other metals. Figure 6c demonstrates the Ni leaching efficiency. At 0.5 vol % H₂O₂, the Ni leaching efficiency increased by approximately 60% within 10 min and continued

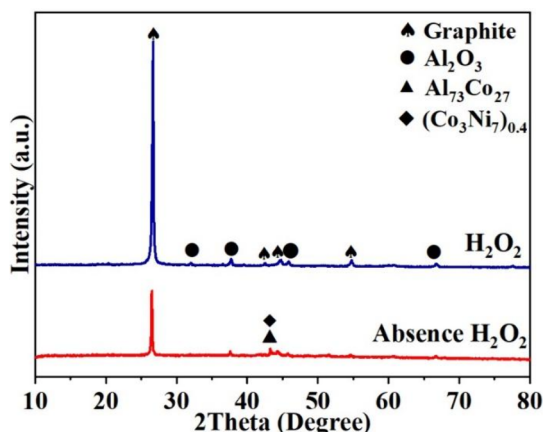


Figure 9. XRD patterns of leaching residues with 1 M H_2SO_4 and a S/L ratio of 10 g/200 mL at 60 °C for 120 min, with and without H_2O_2 .

to increase steadily, reaching 72% at 120 min. At higher H_2O_2 concentrations (1–2 vol %), the Ni leaching efficiency reached 90% within 10 min, slightly increasing to approximately 97% at 120 min. **Figure 6d** presents the Co leaching efficiency. At 0.5 vol % H_2O_2 , the Co leaching efficiency increased by 60% within 10 min and then slightly increased to approximately 65% at 120 min. At higher H_2O_2 concentrations (1–2 vol %), the Co leaching efficiency increased to 80% within 10 min and then slightly increased to approximately 83% at 120 min. Therefore, a higher H_2O_2 concentration (1–2 vol %) substantially enhanced the metal leaching efficiency compared to that in the absence of H_2O_2 . Adding H_2O_2 changed the valence states of the metal ions, breaking metal–oxygen and metal–metal bonds, thereby increasing the leaching rates and greatly improving Ni and Co leaching efficiencies.⁴² In general, H_2O_2 can exhibit dual redox behavior in acidic solutions, acting as an oxidizing and/or reducing agent, as illustrated in **eqs 2** and **3**.⁴³



However, the calcined black mass used in this study presents a unique redox profile compared to the original $\text{Li}_{x}\text{Mn}_y\text{Co}_z\text{O}_2$ cathode materials.^{29,44} For instance, Ni was

present in oxidation states ranging from 0 to 2+, Co predominantly existed in the 0 oxidation state, and Mn primarily resided in the 2+ oxidation state for the starting material (as confirmed by XAS analysis, **Figure 2**). In this context, H_2O_2 functions as an oxidizing agent, promoting the oxidation of these metals to their cationic forms, thereby enhancing the leaching process. The optimal conditions determined from these experiments was 1 vol % H_2O_2 for 120 min, resulting in Li, Mn, Ni, and Co leaching efficiencies of 100%, 100%, 94.39%, and 83.36%, respectively. However, the Co leaching efficiency remained less than 85%. Therefore, further investigation was conducted to determine the combined effect of H_2O_2 concentration and temperature on metal leaching efficiency.

The effect of changing the temperature of the leaching solution between 30 and 70 °C was investigated in order to optimize the leaching efficiency of black mass from the spent LIBs. Data was recorded at every interval of 10 °C, and H_2O_2 concentration was fixed at 1 vol %. The results showed that at 60 °C, the target metals were close to being completely leached (Li, Mn, and Ni, with Co approaching 100%), as depicted in **Figure 7**. Therefore, the optimal conditions for leaching the target metals from the black mass were 1 M H_2SO_4 , 1% H_2O_2 , and a S/L ratio of 50 g/L at 60 °C for 60 min, resulting in leaching efficiencies of 100% for Li, Mn, and Ni, and 97.17% for Co, respectively.

3.3. Kinetic Analysis of the Leaching Process.

3.3.1. Kinetic Analysis. This study investigated the leaching kinetics of Li, Ni, Mn, and Co from spent LIBs using 1 M H_2SO_4 with H_2O_2 added as the additive. Leaching experiments were conducted at various time intervals (0–35 min) and temperatures (30 °C–70 °C), with a fixed acid concentration (1 M H_2SO_4), H_2O_2 content (1 vol %), and S/L ratio (50 g/L). The resulting data were employed to evaluate and compare the fitting efficacies of the shrinking core and Avrami models to describe the metal leaching kinetics. The shrinking core model consists of two distinct equations: chemical reactions controlled by surface chemical reactions (**eq 4**) and diffusion (**eq 5**). The Avrami model (**eq 6**) is employed in the study of multi metal leaching, representing solid–liquid phase transformations or a mixed kinetic model that incorporates surface chemical reaction and diffusion control.^{45,46}

$$1 - (1 - X)^{1/3} = Kt \quad (4)$$

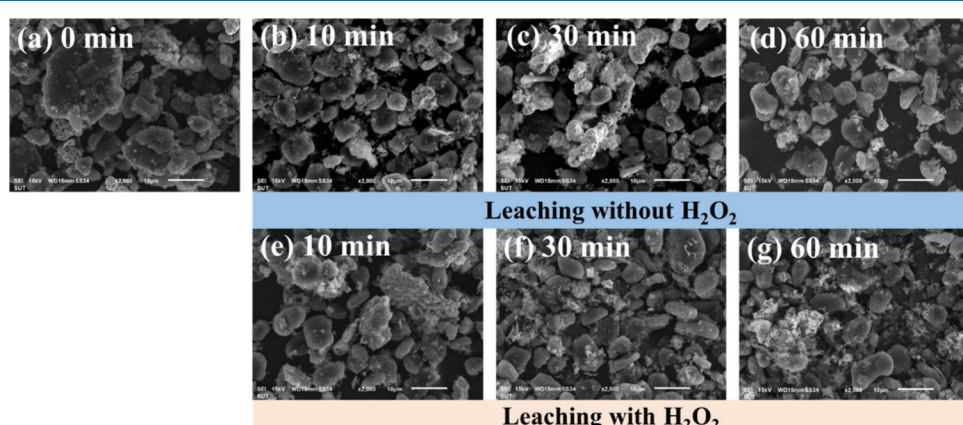


Figure 10. SEM images of leaching residues: without H_2O_2 at (a) 0 min, (b) 10 min, (c) 30 min, and (d) 60 min; with H_2O_2 at (e) 10 min, (f) 30 min, and (g) 60 min.

$$1 - 3(1 - X)^{2/3} + 2(1 - X) = Kt \quad (5)$$

$$\ln(-\ln(1 - X)) = \ln K + n \ln t \quad (6)$$

where X represents the metal leaching efficiency, K is the reaction constant, t is the reaction time (in min), and n is the reaction order. The experimental data were fitted to the kinetic models to assess their suitability. A lower coefficient of determination (R^2 value) indicated a poor fit, suggesting that the model did not accurately represent the data, whereas a higher R^2 value indicated a better fit, ensuring the precision and reliability of the experimental results.

The activation energy (E_a), as determined by the Arrhenius eq (eq 7), elucidates the correlation between the rate constant of a chemical reaction and temperature:

$$K = A e^{-E_a/(RT)} \quad (7)$$

where K is the rate constant of the chemical reaction, T is the temperature, A is the frequency factor, E_a is the activation energy, and R is the universal gas constant ($8.314 \text{ J mol}^{-1} \text{ K}^{-1}$). To experimentally determine E_a , the Arrhenius plot involves plotting $\ln K$ against $1/T$. The resulting linear slope from this plot is denoted as $-E_a/R$.

The leaching kinetics of Li, Ni, and Co at varying temperatures were analyzed using the shrinking core and Avrami models (Figure 8), focusing on the initial 10 min of leaching with H_2O_2 due to the potential for complete Li and Ni dissolution within this time frame. The Mn leaching data are omitted due to its rapid dissolution in the acidic media, which was attributed to the cubic arrangement of MnO (confirmed by XRD (Figure 1c) and XAS (Figure 2e)) facilitating high solubility and rapid reactions with the leaching and additives.⁴⁷ By contrast, Co leaching exhibited a slower process, necessitating data collection for up to 60 min. As shown in Figure 8a–c, the Avrami model effectively described the leaching mechanisms for Li, Co, and Ni, with R^2 values greater than 0.93, suggesting that surface layer diffusion and chemical reaction control played substantial roles in the leaching processes for all three metals. Figure 8d illustrates the apparent E_a values associated with the metal leaching process across different temperature ranges. Specifically, the apparent E_a values were determined to be approximately 7.83 kJ mol^{-1} for Li, 5.08 kJ mol^{-1} Co, and 5.65 kJ mol^{-1} for Ni. Compared to previous research in this field, our work explores the optimization of leaching conditions for the incinerated black mass. By varying the concentration of H_2SO_4 and H_2O_2 at different temperatures, our findings showed significantly lower activation energies than other studies (Table S2), indicating that surface chemical reactions and diffusion controls leaching.^{4,25–27,36,42,48–50} This disparity may be attributed to differences in the initial raw materials and metal oxidation states before leaching.

However, a comparison of the models applicable to the experimental data without H_2O_2 added as an additive, as illustrated in Figures S1 and S2, indicated that the kinetic behaviors of the metals presented notable disparities in the presence of H_2O_2 . The Avrami model exhibited excellent agreement ($R^2 > 0.90$) for Li and Mn leaching, suggesting rapid leaching kinetics that were potentially controlled by a combination of surface layer diffusion and chemical reactions. By contrast, the diffusion-controlled shrinking core model best described the Ni and Co leaching data ($R^2 > 0.90$). This observed difference could be attributed to the lower oxidation

states of Ni and Co, potentially leading to stronger bonding within the cathode material and, consequently, slower leaching rates compared to Li and Mn. Moreover, the E_a values for metal leaching without H_2O_2 were considerably higher than those obtained with H_2O_2 , with values of $9.888 \text{ kJ mol}^{-1}$ for Li, $59.181 \text{ kJ mol}^{-1}$ for Co, $68.657 \text{ kJ mol}^{-1}$ for Ni, and $0.576 \text{ kJ mol}^{-1}$ for Mn. The efficacy of H_2O_2 as an additive is notably evident in its ability to enhance target metal liberation from calcined black mass. This facilitates their subsequent recovery through established selective separation techniques. Several well-documented precipitation processes employing specific pH adjustments and precipitating agents can be effectively utilized for metal recovery from the leached solution. For instance, Ni precipitation can be achieved using either NaOH or Na_2CO_3 , while Co separation can be accomplished with oxalic acid or NaOH . Similarly, Mn recovery can be facilitated by Na_2CO_3 or KMnO_4 precipitation, and Li can be selectively precipitated with Na_2CO_3 or Na_3PO_4 .^{1,12,32,51}

3.3. Characterization of Residues from the Leaching Process. The residues from the leaching process were characterized by XRD analysis, and their morphological characteristics were investigated via SEM-EDS. Comparative analysis was performed on the leaching residues obtained with and without H_2O_2 . Figure 9 presents the XRD patterns of the leaching residues, revealing substantial changes in the spectral peaks. The spectral peaks attributed to LiAlO_2 , MnO , $\text{Al}_{73}\text{Co}_{27}$, $(\text{Co}_3\text{Ni}_7)_{0.4}$, and AlMnNi_6 (Figure 1c) disappeared in the spectra of the leaching residues compared to that of the initial material. Treatment with a leaching solution containing 1 vol % H_2O_2 caused gradual weakening and eventual disappearance of these spectral peaks. Nevertheless, those attributed to graphite and alumina persisted in the spectra of the leaching residues. The leaching process demonstrated selective extraction of valuable metals, while graphite and aluminum compounds were retained in the residual material. The chemical compositions of the residues assessed by ICP-OES, as shown in Table S1, indicated that Li, Mn, and Ni were absent in the leaching residues, suggesting that these elements had leached into the solution. This finding indicated that Li, Ni, Mn, and Co completely reacted with the leaching solution, and their maximum leaching rates were reached. The SEM image of the black mass before leaching showed a smooth surface and asymmetrical, agglomerated shapes (Figure 10a). However, the leaching residues exhibited a reduced particle size following leaching with H_2SO_4 at various intervals, as shown in Figure 10b–d. Upon reaction of the black mass with a leaching solution containing H_2SO_4 with H_2O_2 , metal ions were released into the solution. Figure 10e–g illustrates that H_2O_2 had a disruptive effect on the black mass surface, as the surface of the leaching residues exhibited more holes and defects than those without H_2O_2 treatment. The EDS analysis also confirmed a decrease in the particle size and reduced distribution of Ni, Mn, and Co in the leaching residues, as shown in Figures S3–S6. These results were consistent with the XRD results and further confirmed that leaching for 60 min was, in fact, the optimum leaching time. The XRD and SEM-EDS analysis results of the leaching residues further supported the applicability of the Avrami model to the black mass particles, suggesting that metal leaching was controlled by surface chemical reactions and diffusion.

4. CONCLUSION

This study investigated the leaching behavior of valuable metals (Li, Ni, Mn, Co) from calcined black mass derived from spent LIBs. The optimal leaching conditions using H_2SO_4 achieved high efficiencies for Li and Mn (100%), while Ni and Co exhibited moderate efficiencies (89.13% and 82.23%, respectively). Kinetic analysis revealed diffusion-controlled leaching for Ni and Mn, while Li and Mn followed the Avrami model. Significantly improved leaching efficiencies were achieved by incorporating H_2O_2 . Under these optimized conditions (lower temperature and shorter leaching time), complete leaching of Li, Mn, and Ni and near-complete leaching of Co (97.17%) were obtained. Kinetic studies indicated a shift toward the Avrami model for Li, Ni, and Co leaching with H_2O_2 , suggesting a change in the rate-limiting step. These findings demonstrate the effectiveness of H_2O_2 in enhancing the leaching process for recovering valuable metals from calcined black mass, offering a promising approach for LIB recycling. The enriched leachate obtained using H_2O_2 can be further processed for selective separation of target metals using appropriate techniques.

■ ASSOCIATED CONTENT

Supporting Information

The Supporting Information is available free of charge at <https://pubs.acs.org/doi/10.1021/acsomega.4c05086>.

Fitting of leaching kinetics data for (a) Li and (b) Mn by Avrami model, and (c) Ni and (d) Co by the diffusion-controlled shrinking core model (Figure S1); Arrhenius plot for leaching without H_2O_2 (Figure S2); chemical composition of leaching residues (Table S1); experimental conditions utilized to leach cathode active materials from LIBs (Table S2); EDS mapping analysis of elements in leaching residues without H_2O_2 at 60 °C for 10 min (Figure S3); EDS mapping analysis of elements in leaching residues without H_2O_2 at 60 °C for 60 min (Figure S4); EDS mapping analysis of elements in leaching residues with H_2O_2 at 60 °C for 10 min (Figure S5); EDS mapping analysis of elements in leaching residues with H_2O_2 at 60 °C for 60 min (Figure S6) ([PDF](#))

■ AUTHOR INFORMATION

Corresponding Author

Sakhob Khumkao – School of Metallurgical Engineering, Institute of Engineering, Suranaree University of Technology, Nakhon Ratchasima 30000, Thailand; Email: sakhob@sut.ac.th

Authors

Natcha Wongnaree – School of Metallurgical Engineering, Institute of Engineering, Suranaree University of Technology, Nakhon Ratchasima 30000, Thailand; [ORCID iD](https://orcid.org/0009-0008-0629-4456)

Tapany Patcharawit – School of Metallurgical Engineering, Institute of Engineering, Suranaree University of Technology, Nakhon Ratchasima 30000, Thailand

Tanongsak Yingnakorn – School of Metallurgical Engineering, Institute of Engineering, Suranaree University of Technology, Nakhon Ratchasima 30000, Thailand

Complete contact information is available at:

<https://pubs.acs.org/doi/10.1021/acsomega.4c05086>

Author Contributions

Natcha Wongnaree: conceptualization, methodology, analysis data, writing—original draft. Tapany Patcharawit: conceptualization. Tanongsak Yingnakorn: conceptualization, writing—original draft. Sakhob Khumkao: conceptualization, methodology, supervision, writing—review and editing. All authors have approved the final version.

Notes

The authors declare no competing financial interest.

■ ACKNOWLEDGMENTS

The authors would like to acknowledge the Synchrotron Light Research Institute, Thailand, for providing supportive synchrotron radiation facilities. Our gratitude also extends to the Innovative Processing and Recycling of Metal Research Center at Suranaree University of Technology for supporting this study and providing outstanding facilities and services.

■ REFERENCES

- (1) Chen, W.-S.; Ho, H.-J. Recovery of Valuable Metals from Lithium-Ion Batteries NMC Cathode Waste Materials by Hydrometallurgical Methods. *Metals* **2018**, *8* (5), 321.
- (2) Mossali, E.; Picone, N.; Gentilini, L.; Rodriguez, O.; Pérez, J. M.; Colledani, M. Lithium-Ion Batteries towards Circular Economy: A Literature Review of Opportunities and Issues of Recycling Treatments. *Journal of Environmental Management* **2020**, *264*, 110500.
- (3) Tang, X.; Guo, Q.; Zhou, M.; Zhong, S. Direct Regeneration of LiNi0.5Co0.2Mn0.3O2 Cathode Material from Spent Lithium-Ion Batteries. *Chinese Journal of Chemical Engineering* **2021**, *40*, 278–286.
- (4) Sahu, S.; Devi, N. Two-Step Leaching of Spent Lithium-Ion Batteries and Effective Regeneration of Critical Metals and Graphitic Carbon Employing Hexuronic Acid. *RSC Adv.* **2023**, *13* (11), 7193–7205.
- (5) Guzolu, J. S.; Gharabaghi, M.; Mobin, M.; Alilo, H. Extraction of Li and Co from Li-Ion Batteries by Chemical Methods. *J. Inst. Eng. India Ser. D* **2017**, *98* (1), 43–48.
- (6) Li, J.; Yang, X.; Fu, Y.; Huang, H.; Zhong, Z.; Wang, Y. Recovery of Fe, Mn, Ni and Co in Sulfuric Acid Leaching Liquor of Spent Lithium Ion Batteries for Synthesis of Lithium Ion-Sieve and Ni_xCoyMn_{1-x-y}(OH)₂. *Hydrometallurgy* **2019**, *190*, 105190.
- (7) Prabaharan, G.; Barik, S. P.; Kumar, N.; Kumar, L. Electrochemical Process for Electrode Material of Spent Lithium Ion Batteries. *Waste Management* **2017**, *68*, 527–533.
- (8) Ferreira, D. A.; Prados, L. M. Z.; Majuste, D.; Mansur, M. B. Hydrometallurgical Separation of Aluminum, Cobalt, Copper and Lithium from Spent Li-Ion Batteries. *J. Power Sources* **2009**, *187* (1), 238–246.
- (9) He, H.; Feng, J.; Gao, X.; Fei, X. Selective Separation and Recovery of Lithium, Nickel, MnO₂, and Co₂O₃ from Li-Ni0.5Mn0.3Co0.2O₂ in Spent Battery. *Chemosphere* **2022**, *286*, 131897.
- (10) Sahu, S.; Pati, S.; Devi, N. A Detailed Kinetic Analysis of the Environmentally Friendly Leaching of Spent Lithium-Ion Batteries Using Monocarboxylic Acid. *Metals* **2023**, *13* (5), 947.
- (11) Verma, A.; Corbin, D. R.; Shiflett, M. B. Lithium and Cobalt Recovery for Lithium-Ion Battery Recycle Using an Improved Oxalate Process with Hydrogen Peroxide. *Hydrometallurgy* **2021**, *203*, 105694.
- (12) Nayl, A. A.; Elkhashab, R. A.; Badawy, S. M.; El-Khateeb, M. A. Acid Leaching of Mixed Spent Li-Ion Batteries. *Arabian Journal of Chemistry* **2017**, *10*, S3632–S3639.
- (13) Zhang, X.; Cao, H.; Xie, Y.; Ning, P.; An, H.; You, H.; Nawaz, F. A Closed-Loop Process for Recycling LiNi_{1/3}Co_{1/3}Mn_{1/3}O₂ from the Cathode Scraps of Lithium-Ion Batteries: Process Optimization and Kinetics Analysis. *Sep. Purif. Technol.* **2015**, *150*, 186–195.
- (14) Chen, X.; Yang, C.; Yang, Y.; Ji, H.; Yang, G. Co-Precipitation Preparation of Ni-Co-Mn Ternary Cathode Materials by Using the

- Sources Extracting Directly from Spent Lithium-Ion Batteries. *J. Alloys Compd.* **2022**, *909*, 164691.
- (15) Padwal, C.; Pham, H. D.; Jadhav, S.; Do, T. T.; Nerkar, J.; Hoang, L. T. M.; Kumar Nanjundan, A.; Mundree, S. G.; Dubal, D. P. Deep Eutectic Solvents: Green Approach for Cathode Recycling of Li-Ion Batteries. *Adv. Energy and Sustain. Res.* **2022**, *3* (1), 2100133.
- (16) Colledani, M.; Gentilini, L.; Mossali, E.; Picone, N. A Novel Mechanical Pre-Treatment Process-Chain for the Recycling of Li-Ion Batteries. *CIRP Annals* **2023**, *72* (1), 17–20.
- (17) Yi, C.; Zhou, L.; Wu, X.; Sun, W.; Yi, L.; Yang, Y. Technology for Recycling and Regenerating Graphite from Spent Lithium-Ion Batteries. *Chinese Journal of Chemical Engineering* **2021**, *39*, 37–50.
- (18) Chabbadiya, K.; Srivastava, R. R.; Pathak, P. Two-Step Leaching Process and Kinetics for an Eco-Friendly Recycling of Critical Metals from Spent Li-Ion Batteries. *Journal of Environmental Chemical Engineering* **2021**, *9* (3), 105232.
- (19) Jha, M. K.; Kumari, A.; Jha, A. K.; Kumar, V.; Hait, J.; Pandey, B. D. Recovery of Lithium and Cobalt from Waste Lithium Ion Batteries of Mobile Phone. *Waste Management* **2013**, *33* (9), 1890–1897.
- (20) Setiawan, H.; Petrus, H. T. B. M.; Perdana, I. Reaction Kinetics Modeling for Lithium and Cobalt Recovery from Spent Lithium-Ion Batteries Using Acetic Acid. *Int. J. Miner. Metall. Mater.* **2019**, *26* (1), 98–107.
- (21) Zhang, Y.-C.; Yu, W.-H.; Xu, S.-M. Enhanced Leaching of Metals from Spent Lithium-Ion Batteries by Catalytic Carbothermic Reduction. *Rare Met.* **2023**, *42* (8), 2688–2699.
- (22) Chen, H.; Liu, R.; Long, Q.; Liu, Z. Carbonation Precipitation of Manganese from Electrolytic Manganese Residue Treated by CO₂ with Alkaline Additives. In *Proceedings of the 2015 2nd International Conference on Machinery, Materials Engineering, Chemical Engineering and Biotechnology*; Atlantis Press: Chongqing, China, 2016; DOI: 10.2991/mmeceb-15.2016.142.
- (23) Djoudi, N.; Le Page Mostefa, M.; Muhr, H. Hydrometallurgical Process to Recover Cobalt from Spent Li-Ion Batteries. *Resources* **2021**, *10* (6), 58.
- (24) Zeng, G.; Yao, J.; Liu, C.; Luo, X.; Ji, H.; Mi, X.; Deng, C. Simultaneous Recycling of Critical Metals and Aluminum Foil from Waste LiNi_{1/3}Co_{1/3}Mn_{1/3}O₂ Cathode via Ethylene Glycol-Citric Acid System. *ACS Sustainable Chem. Eng.* **2021**, *9* (48), 16133–16142.
- (25) Gao, W.; Song, J.; Cao, H.; Lin, X.; Zhang, X.; Zheng, X.; Zhang, Y.; Sun, Z. Selective Recovery of Valuable Metals from Spent Lithium-Ion Batteries - Process Development and Kinetics Evaluation. *Journal of Cleaner Production* **2018**, *178*, 833–845.
- (26) Meshram, P.; Pandey, B. D.; Mankhand, T. R. Hydro-metallurgical Processing of Spent Lithium Ion Batteries (LIBs) in the Presence of a Reducing Agent with Emphasis on Kinetics of Leaching. *Chemical Engineering Journal* **2015**, *281*, 418–427.
- (27) He, L.-P.; Sun, S.-Y.; Song, X.-F.; Yu, J.-G. Leaching Process for Recovering Valuable Metals from the LiNi_{1/3}Co_{1/3}Mn_{1/3}O₂ Cathode of Lithium-Ion Batteries. *Waste Management* **2017**, *64*, 171–181.
- (28) Kim, S.; Yang, D.; Rhee, K.; Sohn, J. Recycling Process of Spent Battery Modules in Used Hybrid Electric Vehicles Using Physical/Chemical Treatments. *Res. Chem. Intermed.* **2014**, *40* (7), 2447–2456.
- (29) Vieceli, N.; Benjamasutin, P.; Promphan, R.; Hellström, P.; Paulsson, M.; Petranikova, M. Recycling of Lithium-Ion Batteries: Effect of Hydrogen Peroxide and a Dosing Method on the Leaching of LCO, NMC Oxides, and Industrial Black Mass. *ACS Sustainable Chem. Eng.* **2023**, *11* (26), 9662–9673.
- (30) Chen, M.; Ma, X.; Chen, B.; Arsenault, R.; Karlson, P.; Simon, N.; Wang, Y. Recycling End-of-Life Electric Vehicle Lithium-Ion Batteries. *Joule* **2019**, *3* (11), 2622–2646.
- (31) Meshram, P.; Abhilash; Pandey, B. D.; Mankhand, T. R.; Deveci, H. Comparison of Different Reductants in Leaching of Spent Lithium Ion Batteries. *JOM* **2016**, *68* (10), 2613–2623.
- (32) Chen, X.; Xu, B.; Zhou, T.; Liu, D.; Hu, H.; Fan, S. Separation and Recovery of Metal Values from Leaching Liquor of Mixed-Type of Spent Lithium-Ion Batteries. *Sep. Purif. Technol.* **2015**, *144*, 197–205.
- (33) Ebrahimzade, H.; Khayati, G. R.; Schaffie, M. Leaching Kinetics of Valuable Metals from Waste Li-Ion Batteries Using Neural Network Approach. *J. Mater. Cycles Waste Manag.* **2018**, *20* (4), 2117–2129.
- (34) Pinna, E. G.; Drajlin, D. S.; Toro, N.; Rodriguez, M. H. Kinetic Modeling of the Leaching of LiCoO₂ with Phosphoric Acid. *Journal of Materials Research and Technology* **2020**, *9* (6), 14017–14028.
- (35) Wang, Y.; An, N.; Wen, L.; Wang, L.; Jiang, X.; Hou, F.; Yin, Y.; Liang, J. Recent Progress on the Recycling Technology of Li-Ion Batteries. *Journal of Energy Chemistry* **2021**, *55*, 391–419.
- (36) Yang, C.; Wang, J.; Yang, P.; He, Y.; Wang, S.; Zhao, P.; Wang, H. Recovery of Valuable Metals from Spent LiNi_{0.8}Co_{0.1}Mn_{0.1}O₂ Cathode Materials Using Compound Leaching Agents of Sulfuric Acid and Oxalic Acid. *Sustainability* **2022**, *14* (21), 14169.
- (37) Bae, H.; Kim, Y. Technologies of Lithium Recycling from Waste Lithium Ion Batteries: A Review. *Mater. Adv.* **2021**, *2* (10), 3234–3250.
- (38) Jena, K. K.; AlFantazi, A.; Choi, D. S.; Liao, K.; Mayyas, A. Recycling Spent Lithium Ion Batteries and Separation of Cathode Active Materials: Structural Stability, Morphology Regularity, and Waste Management. *Ind. Eng. Chem. Res.* **2024**, *63* (8), 3483–3490.
- (39) Babanejad, S.; Ahmed, H.; Andersson, C.; Samuelsson, C.; Lennartsson, A.; Hall, B.; Arnerlöf, L. High-Temperature Behavior of Spent Li-Ion Battery Black Mass in Inert Atmosphere. *J. Sustain. Metall.* **2022**, *8* (1), 566–581.
- (40) Yang, Y.; Huang, G.; Xu, S.; He, Y.; Liu, X. Thermal Treatment Process for the Recovery of Valuable Metals from Spent Lithium-Ion Batteries. *Hydrometallurgy* **2016**, *165*, 390–396.
- (41) Kwon, O.; Sohn, I. Fundamental Thermokinetic Study of a Sustainable Lithium-Ion Battery Pyrometallurgical Recycling Process. *Resources, Conservation and Recycling* **2020**, *158*, 104809.
- (42) Sun, C.; Xu, L.; Chen, X.; Qiu, T.; Zhou, T. Sustainable Recovery of Valuable Metals from Spent Lithium-Ion Batteries Using DL-Malic Acid: Leaching and Kinetics Aspect. *Waste Manag. Res.* **2018**, *36* (2), 113–120.
- (43) He, L.-P.; Sun, S.-Y.; Song, X.-F.; Yu, J.-G. Leaching Process for Recovering Valuable Metals from the LiNi_{1/3}Co_{1/3}Mn_{1/3}O₂ Cathode of Lithium-Ion Batteries. *Waste Management* **2017**, *64*, 171–181.
- (44) Zou, Y.; Chernyaev, A.; Ossama, M.; Seisko, S.; Lundström, M. Leaching of NMC Industrial Black Mass in the Presence of LFP. *Sci. Rep.* **2024**, *14* (1), 10818.
- (45) Wang, K.; Zhang, G.; Luo, M. Recovery of Valuable Metals from Cathode–Anode Mixed Materials of Spent Lithium-Ion Batteries Using Organic Acids. *Separations* **2022**, *9* (9), 259.
- (46) Xuan, W.; De Souza Braga, A.; Korbel, C.; Chagnes, A. New Insights in the Leaching Kinetics of Cathodic Materials in Acidic Chloride Media for Lithium-Ion Battery Recycling. *Hydrometallurgy* **2021**, *204*, 105705.
- (47) Sinha, M. K.; Purcell, W. Reducing Agents in the Leaching of Manganese Ores: A Comprehensive Review. *Hydrometallurgy* **2019**, *187*, 168–186.
- (48) Meng, F.; Liu, Q.; Kim, R.; Wang, J.; Liu, G.; Ghahreman, A. Selective Recovery of Valuable Metals from Industrial Waste Lithium-Ion Batteries Using Citric Acid under Reductive Conditions: Leaching Optimization and Kinetic Analysis. *Hydrometallurgy* **2020**, *191*, 105160.
- (49) Fan, E.; Yang, J.; Huang, Y.; Lin, J.; Arshad, F.; Wu, F.; Li, L.; Chen, R. Leaching Mechanisms of Recycling Valuable Metals from Spent Lithium-Ion Batteries by a Malonic Acid-Based Leaching System. *ACS Appl. Energy Mater.* **2020**, *3* (9), 8532–8542.
- (50) Gerold, E.; Lerchbammer, R.; Antrekowitsch, H. Recovery of Cobalt, Nickel, and Lithium from Spent Lithium-Ion Batteries with Gluconic Acid Leaching Process: Kinetics Study. *Batteries* **2024**, *10* (4), 120.
- (51) Wongnaree, N.; Sriklang, L.; Kansomket, C.; Chandakhiaw, T.; Patcharawit, T.; Khumkao, S. Precipitation of Lithium Phosphate

from Cathode Materials of Spent Lithium-Ion Battery by Hydro-metallurgy Process. *MSF* **2023**, *1099*, 175–180.